Phytopathology Research

RESEARCH

Open Access

Comparative genomic analysis of three *Enterobacter* strains associated with rice leaf wilt disease

Fei Fu[1†], Xingyu Yu[1†], Xiaojing Lin[1†], Jianhao Lin[1], Yang Xue[1], Ming Hu[1,2], Huilin Chen[1], Yizhen Deng[1], Gan Sha[1], Tong Zhang[1], Xiaofan Zhou[1], Xuefeng Qu[3] and Jianuan Zhou[1*]

Abstract

Recent studies have revealed that certain *Enterobacter* species can induce rice leaf blight symptoms resembling those caused by *Xanthomonas oryzae* pv. *oryzae*, the primary etiological agent of bacterial blight, which poses a significant threat to global rice production. In this study, we refer to the leaf blight caused by *Enterobacter* as rice bacterial leaf wilt to differentiate it from other diseases. To understand the pathogenic mechanisms of these emerging pathogens, we sequenced the complete genomes of three representative *Enterobacter* spp. strains, designated FY158, RG1, and SC1, and performed comprehensively comparative genomic analyses. Our findings reveal that strains FY158 and SC1, respectively isolated from Zhejiang and Sichuan Provinces, both belong to *E. pseudoroggenkampii*, a species previously known only from clinical samples. Strain RG1 isolated from Guangdong Province shares the closest phylogenetic relationship with *E. asburiae*. Moreover, we found that the secondary metabolites aryl polyenes, aerobactin, and enterobactin are associated with the pathogenicity of these *Enterobacter* strains on rice. The complete genome sequences provide a solid foundation for investigating the pathogenic processes of *Enterobacter* spp. associated with rice leaf wilt, and also contribute to the comparative genomic understanding of the genus *Enterobacter*.

Keywords Rice bacterial wilt, *Enterobacter*, Genomic comparison, Virulence

Background

Rice, a globally significant staple crop that feeds over half of the world's population (Huang et al. 2012), is predominantly cultivated in tropical and subtropical regions where it faces persistent threats from various pathogenic microorganisms (Baker et al. 1992; Liu et al. 2014). Among these pathogens, *Xanthomonas oryzae* pv. *oryzae* (*Xoo*)-induced bacterial blight (BB) represents one of the most devastating diseases, capable of causing severe yield losses up to 50% by impairing rice growth and reproductive development (Liu et al. 2014). First documented in 1884 in Japan's Fukuoka region, BB was introduced to China in the 1930s and had spread across ten southern provinces by the end of the 1950s (Mew 1993). Today, this disease has become endemic in virtually all rice-growing regions worldwide (Naqvi 2019).

The canonical pathogen *Xoo*, identified in 1911 (Mizukami and Wakimoto 1969), typically invades rice leaves through hydathodes or wounds, colonizing the intercellular spaces of the underlying epithelium before spreading

[†]Fei Fu, Xingyu Yu, and Xiaojing Lin contributed equally to this work.

*Correspondence:
Jianuan Zhou
jianuanzhou@scau.edu.cn
[1] National Key Laboratory of Green Pesticide, Guangdong Provincial Key Laboratory of Microbial Signals and Disease Control, Engineering Research Center of Biological Control, Ministry of Education, Integrative Microbiology Research Center, South China Agricultural University, Guangzhou 510642, China
[2] Henry Fok School of Biology and Agriculture, Shaoguan University, Shaoguan 512005, China
[3] Dongguan Research Center of Agricultural Sciences, Dongguan 523061, China

systemically through xylem vessels. The bacterium then moves through the veins of leaves and spreads throughout the plant. This infection process manifests as characteristic water-soaked lesions at the leaf tips and margins progressing to chlorotic and necrotic tannish-gray to white streaks along the leaf veins with distinct margins (Lee et al. 2011). During recent field surveys, we collected multiple samples of symptomatic rice leaves showing blight-like symptoms similar to those caused by *Xoo*. However, despite repeated attempts, we failed to isolate *Xoo* from these samples. Instead, our isolation consistently yielded bacterial colonies identified as *Enterobacter* spp. or *Pantoea ananatis* (Xue et al. 2021; Yu et al. 2022).

Enterobacter spp., Gram-negative facultative anaerobes of the ESKAPE group, are primarily recognized as nosocomial pathogens in clinical settings (Davin-Regli et al. 2019). Since the genus was first established in 1960, 22 species have been identified, which are commonly found in soil and water, many exhibiting opportunistic pathogenicity in both animals and plants. Notable plant-associated species include *E. mori* (Zhu et al. 2011; Ahmad et al. 2021; Zhang et al. 2021), *E. cloacae* (Schroeder et al. 2010; Zaid et al. 2011; Cosmas et al. 2016; Li et al. 2022), *E. ludwigii* (Hoffmann et al. 2005), and *E. asburiae* (Lau et al. 2014; Cao et al. 2021; Xue et al. 2021). Despite these observations, the molecular mechanisms underlying the pathogenicity of *Enterobacter* to plants remain poorly understood due to limited research focus.

The advent of genomic technologies has revolutionized bacterial pathogen research, enabling comprehensive analysis of virulence determinants and pathogenic mechanisms (Liu et al. 2016). Leveraging this approach, in this study, we sequenced three *Enterobacter* strains isolated from infected rice plants in Sichuan, Guangdong, and Zhejiang provinces in China. Through comparative genomics and functional annotation, we identified aryl polyenes, aerobactin, and enterobactin produced by strains SC1 and RG1 as key virulence factors contributing to rice leaf wilt. These findings lay a crucial foundation for understanding the role *of Enterobacter* spp. in plant disease and developing targeted control strategies.

Results

The three *Enterobacter* strains exhibit varying pathogenicity toward rice seedlings

Rice seedlings inoculated with the three *Enterobacter* strains displayed symptoms similar to those caused by the typical rice bacterial blight pathogen *Xoo* PXO99^{A}, except that the lesions caused by the former appeared as inverted V-shapes, while those caused by the latter were elongated V-shapes (Fig. 1a). Initially, water-soaked lesions appeared at the leaf tips and margins, followed by rapid expansion into yellowish-brown to tannish-gray lesions with clearly defined edges. Among the tested strains, PXO99^{A} was the most aggressive, while RG1, SC1, and FY158 showed slower disease progression, with RG1 being more virulent than SC1 and FY158 (Fig. 1b).

To determine whether the observed differences in virulence were attributed to variations in growth rate, we assessed the growth curves of these strains in LB and NA media. The results revealed comparable growth rates among the three *Enterobacter* strains, with faster proliferation in LB than in NA. In contrast, *Xoo* PXO99^{A} exhibited significantly lower growth in both media (Additional file 1: Figure S1). These findings suggest that the differential pathogenicity of these strains is primarily determined by their inherent virulence rather than growth kinetics.

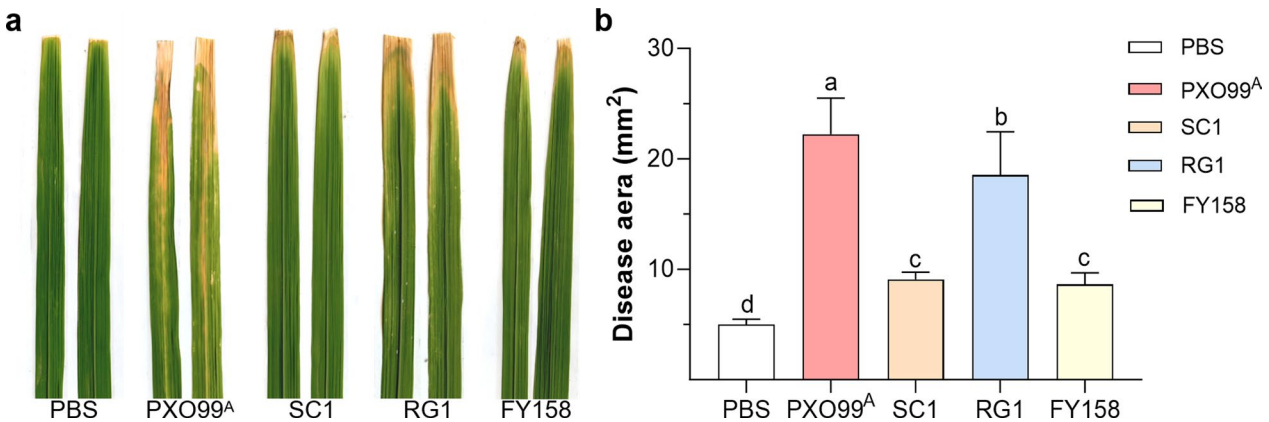

Fig. 1 Pathogenicity of strains FY158, RG1, and SC1 on rice (cv. Yuexiangzhan) leaves. **a** Symptoms on the rice leaves after 15 days post-inoculation (dpi); **b** Diseased area on rice leaves inoculated with the tested strains. Different lowercase letters indicate significant differences ($P < 0.05$)

Biochemical and fatty acid analyses of the three *Enterobacter* strains

As demonstrated in Additional file 2: Table S1, all three *Enterobacter* strains exhibited viability in 4% NaCl, but only strain FY158 (collected from Zhejiang Province) survived in 8% NaCl. Strains FY158 and SC1 displayed distinct carbon source utilization patterns compared to RG1. Specifically, FY158 and SC1 were capable of metabolizing β-Methyl-D-Glucoside, Fusidic Acid, L-Aspartic Acid, D-Salicin, and L-Glutamic Acid, whereas RG1 showed only weak or no activity for these substrates. Conversely, RG1 was positive for Methyl Pyruvate, while FY158 and SC1 exhibited minimal response. Notably, despite belonging to the same species (see the section below), FY158 and SC1 also differed in their carbon source utilization profiles. FY158 could metabolize D-Maltose, D-Raffinose, D-Melibiose, and L-Rhamnose, whereas SC1 and RG1 could not. Conversely, FY158 was unable to utilize D-Serine, N-Acetyl-β-D-Mannosamine, and N-Acetyl-D-Galactosamine, while SC1 and RG1 showed positive reactions for these compounds.

Chemotaxonomic analysis showed that the major cellular fatty acids (> 5%) in strains FY158, RG1, and SC1 included summed feature 3 (10.82%, 12.49%, and 4.12%, respectively, consisting of C16:1ω7c and/or C16:1ω6c), C17:1 ω8c (0.74%, 1.12%, and 0.51%, respectively), summed feature 8 (27.23%, 34.50%, and 24.99%, respectively, comprising C18:1ω7c and/or C18:1ω6c), summed feature 2 (7.33%, 7.10%, and 6.56%, respectively, including C14:0 3-OH, iso-C16:1 I, and/or C12:0 aldehyde), and C15:0 3-OH (0.40%, 0.26%, and 0.56%, respectively) (Additional file 2: Table S1).

Strains SC1 and RG1 exhibit a broader antibacterial spectrum

To investigate the differences in virulence among the strains, we analyzed their production of virulence factors. The results revealed that all tested strains exhibited weak pectin lyase (Pel) enzyme activity. While the three *Enterobacter* strains produced no detectable polygalacturonase (Peh), protease (Prt), or cellulase (Cel) enzymes, *Xoo* PXO99^{A} was capable of producing Prt and Cel. Notably, SC1 and RG1 inhibited the growth of *Es. coli* DH5α (Fig. 2a). FY158 strain demonstrated slightly faster swimming and swarming motility than the other two *Enterobacter* strains, but obviously less biofilms, whereas PXO99^{A} failed to produce biofilms altogether (Fig. 2b).

To evaluate the antimicrobial spectrum of SC1 and RG1, we tested their activity against various bacterial and fungal strains, including two *Bacillus* strains, three *Enterobacter* strains in this study, two *P. anantis* strains (SC7 and MX3, previously isolated from diseased rice leaves) (Xue et al. 2021), two *Dickeya* strains, two *Xanthomonas* strains, *Rhizoctonia solani* AG-1 1A, and *Magnaporthe oryzae* B157. The results showed that SC1 inhibited the growth of *Bacillus*, while both SC1 and RG1 suppressed the growth of *Dickeya* and *Xanthomonas* strains. In contrast, FY158 showed only minimal inhibitory effects on *Xanthomonas*, and none of the *Enterobacter* strains inhibited fungal growth. Additionally, all three *Enterobacter* strains demonstrated resistance to their own antibacterial metabolites (Fig. 2c).

SC1 and FY158 were identified as *E. pseudoroggenkampii*, while RG1 was classified as *E. asburiae*

To elucidate the molecular basis of their pathogenicity, we sequenced the genomes of strains SC1, RG1, and FY158 using both Nanopore PromethION and Illumina NovaSeq platforms. All three assemblies yielded complete circular chromosomes without gaps or plasmids (Additional file 1: Figure S2), with the following genomic features: sizes of 4,814,123 bp (SC1), 4,583,407 bp (RG1), and 4,730,290 bp (FY158); GC contents of 55.72%, 55.96%, and 55.61%; protein-coding genes numbering 4521, 4257, and 4432; and RNA genes totaling 118, 116, and 115, respectively. Each strain contained 25 rRNA genes, while pseudogene counts were higher in SC1 and FY158 (55 and 50) compared to RG1 (38) (Table 1).

For taxonomic classifications, we calculated average nucleotide identity (ANI) values among the three strains and 23 reference *Enterobacter* genomes. SC1 showed close relatedness to FY158 (ANI 98.41%, Additional file 2: Table S2). FY158 exhibited strong similarity to *E. pseudoroggenkampii* 155,092 (GCF_026420145.1 human isolate from China) with ANI 98.40% and digital DNA-DNA hybridization (dDDH) 92.20%, both exceeding established species thresholds (ANI ≥ 95%, dDDH ≥ 70%), confirming SC1 and FY158 as *E. pseudoroggenkampii*. RG1's closest match was *E. asburiae* 17Nkhm-UP2 (GCF_007035805.1) with ANI 98.36% and dDDH 91.50%, supporting its classification as *E. asburiae*.

Phylogenomic analysis of the three strains, along with representative *Enterobacter* species, further validated this classification. The phylogenetic tree demonstrated that FY158 and reference strain *E. pseudoroggenkampii* 155,092 formed a monophyletic clade with SC1, while RG1 clustered closely with *E. asburiae* 17Nkhm-UP2. All other *Enterobacter* species showed significantly greater evolutionary distances from these strains (Fig. 3).

Comparative genomics revealed substantial divergence among the three strains

To further investigate the function differences at the genetic level, we performed BLAST analysis of these genomic sequences against multiple functional

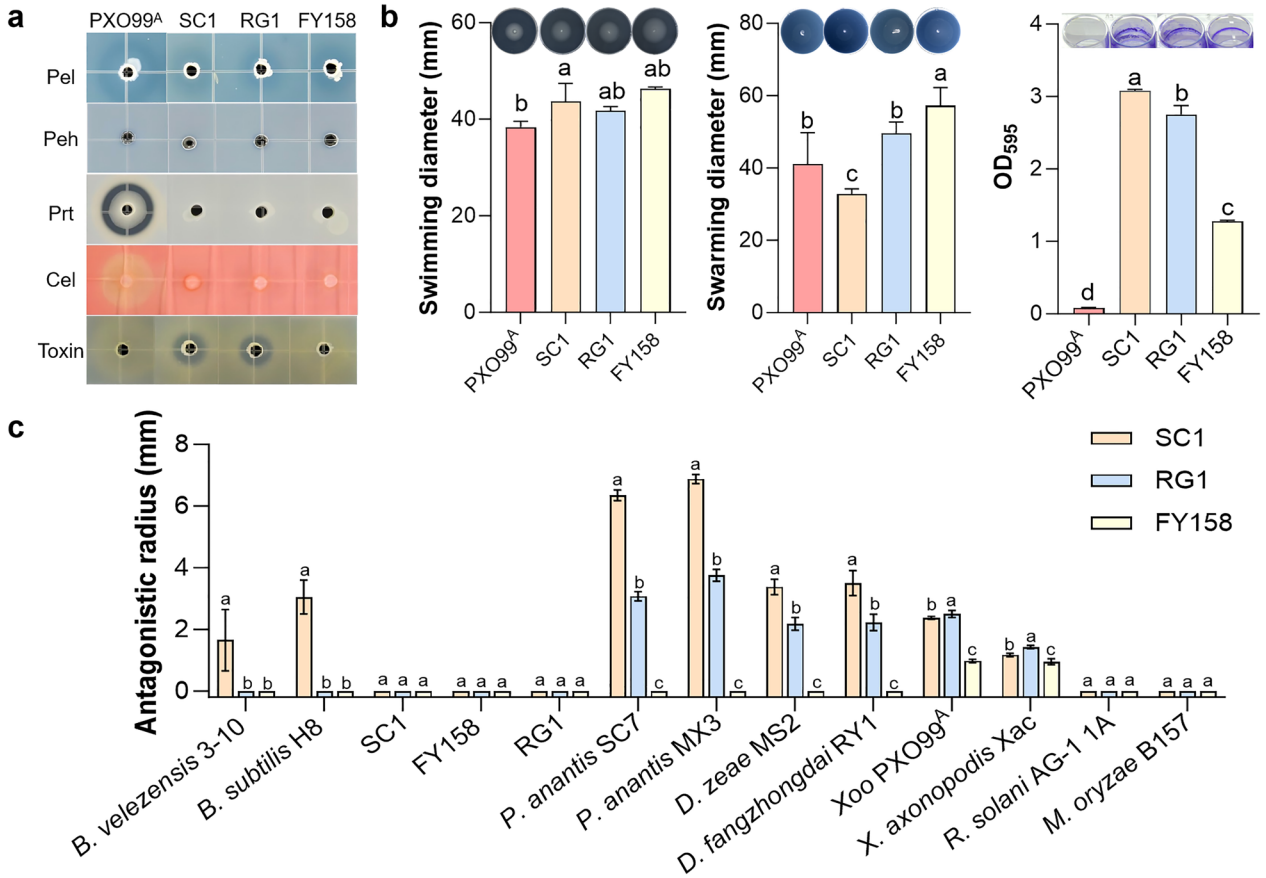

Fig. 2 Cell wall degrading enzymatic activity, motility, biofilm formation, and antimicrobial activity of strains PXO99^{A}, SC1, RG1, and FY158. **a** Plant cell wall degrading enzymes and phytotoxins produced by the tested strains; **b** Bacterial swimming, swarming motility, and biofilm formation of the tested strains. Different lowercase letters indicate significant differences ($P < 0.05$). **c** The inhibitory effects of the tested strains against bacteria and fungi

Table 1 Genomic features of SC1, RG1, and FY158

Features	SC1	RG1	FY158
Genome Size (bp)	4,814,123	4,583,407	4,730,290
GC content (%)	55.72	55.96	55.61
Genes (total)	4639	4373	4547
CDSs (total)	4521	4257	4432
RNA genes	118	116	115
rRNA (5S, 16S, & 23S)	9, 8, 8	9, 8, 8	9, 8, 8
tRNA	84	83	83
ncRNA	9	8	7
Pseudogenes	55	38	50
CRISPR	4	5	6

databases, including nr, eggNOG, GO, KEGG, and Swiss-Prot. The functional annotation results are summarized in Additional file 2: Table S3. Specifically, 4113, 4171, and 4348 predicted genes from strains SC1, RG1, and FY158, respectively, were annotated in the nr database. For the GO and Swiss-Prot databases, the corresponding gene counts were 2566, 3361, and 3556 (GO), and 4431, 3453, and 3540 (Swiss-Prot). Approximately 2900 genes were associated with metabolic pathways based on KEGG annotation (Additional file 2: Table S3). Notably, despite both being *E. pseudoroggenkampii* species, SC1 and FY158 exhibited significant variation in the number of functionally annotated genes.

To explore potential pathogenic mechanisms, we compared the annotated proteins of all three strains against the Virulence Factor Database (VFDB). This analysis identified 162 putative virulence factors in strains FY158 and RG1, and 124 in SC1 (BLASTp hits with e-value < 1e−20, identity ≥ 50%, and coverage ≥ 70%) (Additional file 3: Table S4). Predicted virulence-related gene clusters included those encoding Type I fimbriae, curli, flagella, capsule and Type VI secretion system (T6SS), as well as biosynthetic pathways for the secondary metabolites enterobactin (*ent*) and

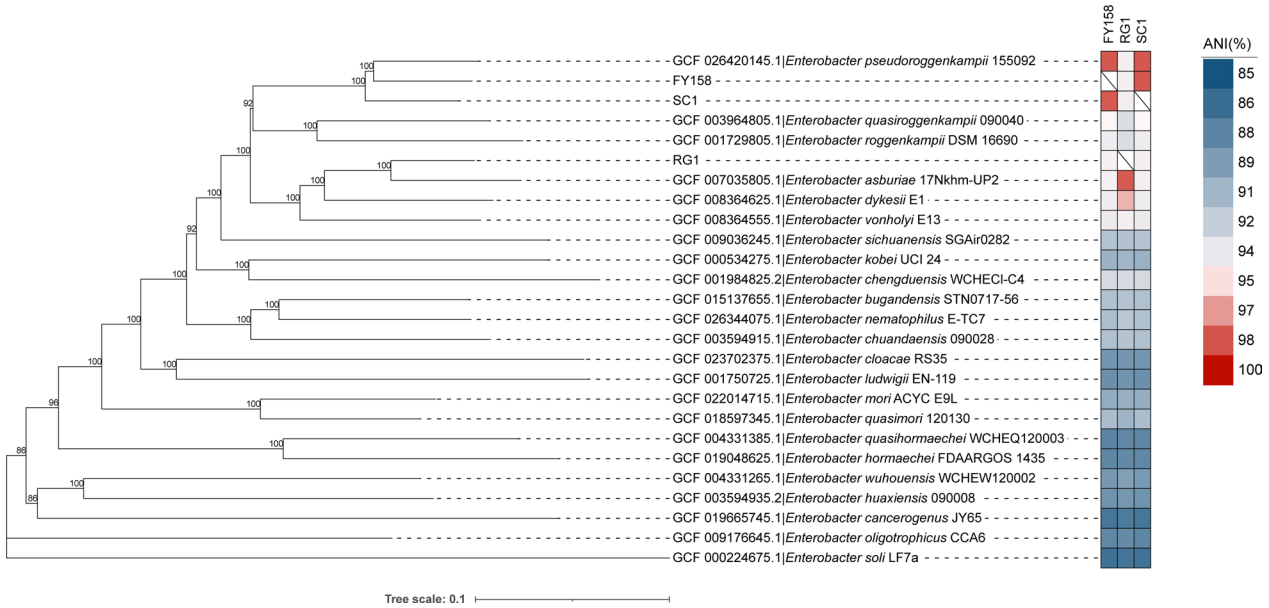

Fig. 3 Phylogenetic relationships among the three *Enterobacter* strains and the 23 recognized *Enterobacter* species. The phylogeny is a maximum-likelihood tree inferred using IQ-TREE. All internal branches in the tree received 100% bootstrap support. A heatmap of the ANI values between FY158/RG1/SC1 and the 23 representative *Enterobacter* strains is shown on the right of the tree

aerobactin (*iuc*). Notably, SC1 lacked the capsule-coding gene cluster (Additional file 3: Table S4).

Orthologous gene analysis reveals strain-specific features

Comparative genomics further delineated unique genetic traits among the strains. Orthologous gene cluster analysis identified 15 SC1-specific genes, including four encoding hypothetical proteins, three SUMF1/EgtB/PvdO family non-heme iron enzymes, two VgrG (T6SS tip protein), two FRG domain-containing proteins, two lysis proteins, and two PAAR domain proteins. Strain FY158 harbored nine unique genes, comprising five T6SS-associated genes, two hypothetical proteins, and two phosphotransferase system-related genes. In contrast, RG1 exhibited the highest genetic distinctiveness, with 45 unique genes: 12 hypothetical proteins, 10 helix-turn-helix (HTH) domain proteins, four RelE/ParE family type II toxin-antitoxin system toxins, one T6SS protein Rhs, four AAA-family ATPases, four ASCH domain proteins, four HTH-type transcriptional regulators, two eCbtA-family toxin-antitoxin toxins, two bacteriophage defense1 site-specific integrases, and one tyrosine-type recombinase/integrase (Additional file 2: Table S5).

Pathogenomics analysis reveals that aryl polyenes, aerobactin, and enterobactin siderophores likely serve as major virulence factors in *Enterobacter* spp. infecting rice plants

To investigate virulence-associated factors, we first examined the distribution of genes encoding secretion systems across the three *Enterobacter* strains. Our analysis showed that FY158 and SC1 harbor five secretion systems: Type I (T1SS), Type II (T2SS), Type IV (T4aP), Type V (T5SS), and Type VI (T6SSi). In contrast, RG1 has only three systems (T2SS, T5SS, and T6SSi). Importantly, all three strains lack the Type III secretion system (T3SS) (Table 2).

Secretion system characterization

T1SS: FY158 and SC1 share conserved T1SS components, including an ABC endomembrane transporter, a periplasmic membrane fusion protein (MFP), and an outer-membrane pore protein (OMF), which collectively facilitate substrate translocation across the bacterial cell envelope. RG1 lacks these homologs.

T2SS: All three strains harbor the core *gspDEFHIJKMO* genes. Additionally, FY158 carries *gspL*, while SC1 possesses *gslCGL*.

T4aP: FY158 and SC1 encode the type IV pilus machinery (*pilABCT*, *gspO*), with FY158 also containing *pilMQ*. No T4SS-related genes were detected in RG1.

T5SS: SC1 encodes two autotransporter domain-containing proteins, two ShlB/FhaC/HecB-family hemolysin secretion/activation proteins, and one YadA C-terminal domain-containing protein. FY158 carries an additional ShlB/FhaC/HecB-family protein, whereas RG1 possesses one more autotransporter domain-containing protein and two more ShlB/FhaC/HecB-family proteins.

Table 2 List of hit genes encoding secretion systems in the three strains

Model	Genes in FY158	Genes in RG1	Genes in SC1
T1SS	*omf**2, *mfp*, *abc*	–	*omf*, *mfp*, *abc*
T2SS	*gspD*, *gspE*, *gspF*, *gspH*, *gspI*, *gspJ*, *gspK*, *gspL*, *gspM*, *gspO*	*gspD*, *gspE*, *gspF*, *gspH*, *gspI*, *gspJ*, *gspK*, *gspM*, *gspO*	*gspC*, *gspD*, *gspE*, *gspF*, *gspG*, *gspH*, *gspI*, *gspJ*, *gspK*, *gspL*, *gspM*, *gspO*
T4aP	*pilA*, *pilB*, *pilC*, *pilM*, *pilQ*, *pilT*, *gspO*	–	*pilA*, *pilB*, *pilC*, *pilT*, *gspO*
T5aSS	*T5aSS_PF03797**2	T5aSS_PF03797*3	T5aSS_PF03797*2
T5bSS	T5bSS_translocator*3	T5bSS_translocator*4	T5bSS_translocator*2
T5cSS	T5cSS_PF03895	T5cSS_PF03895	T5cSS_PF03895
T6SSi	*evpJ**2, *tssA*, *tssB*, *tssC*, *tssD*, *tssE*, *tssF*, *tssG*, *tssH*, *tssJ*, *tssK**2, *tssL*, *tssM*	*evpJ*, *tssA*, *tssB*, *tssC*, *tssD*, *tssE**2, *tssF*, *tssG*, *tssH*, *tssI*, *tssL*, *tssM*	*evpJ**3, *tssA**2, *tssB**2, *tssC**2, *tssD*, *tssE**2, *tssF**2, *tssG**2, *tssH**2, *tssI**2, *tssJ**2, *tssK**2, *tssL*, *tssM**2

"–" Denotes absent in the genome

T6SS: The most striking divergence among strains lies in their T6SS, a system implicated in bacterial competition and pathogenesis (Asolkar and Ramesh 2020). SC1 uniquely harbors two T6SS clusters, while FY158 and RG1 each carry only one (Fig. 4). SC1 retains a full complement of T6SS core genes, whereas RG1 lacks the membrane-associated *TssJ* and the baseplate component *TssK* (Gallegos-Monterrosa et al. 2021). FY158 is deficient in *TssI* (*VgrG*), a critical structural component required for T6SS functionality (Yang et al. 2023).

Antimicrobial activity and secondary metabolites

Consistent with prior findings (Xue et al. 2021), strains SC1 and RG1 exhibited broad-spectrum antibacterial activity against *Es. coli* DH5α, *P. ananatis*, *Dickey* spp., and *Xanthomonas* spp., with strain SC1 also showing mild antagonism toward *Bacillus* spp. In contrast, FY158 displayed only weak inhibition against two *Xanthomonas* strains (Fig. 2a, c). antiSMASH-based analysis identified biosynthetic gene clusters (BGCs) for aerobactin, deschlorosetamycin A, O-antigens, and enterobactin in all three strains. SC1 and RG1 share a BGC for aryl polyenes, while SC1 and FY158 both encoded saquaymycin A. FY158 uniquely harbored the microcin C7 BGC. Among these, only microcin C7, aerobactin, enterobactin and aryl polyene (APE) BGCs exhibited high similarity to known reference clusters (Table 3, Additional file 1: Figure S3).

Functional validation of virulence factors

Strain SC1 exhibits distinctly superior and broader-spectrum antibacterial activity, which suggests a more complex and potent competitive machinery. To elucidate the roles of APEs, aerobactin, and enterobactin, we generated SC1 mutants (Δ*ape*, Δ*entA*, Δ*entC*, Δ*entF*, Δ*iucC*, and Δ*entF*Δ*iucC*). While growth remained unaffected

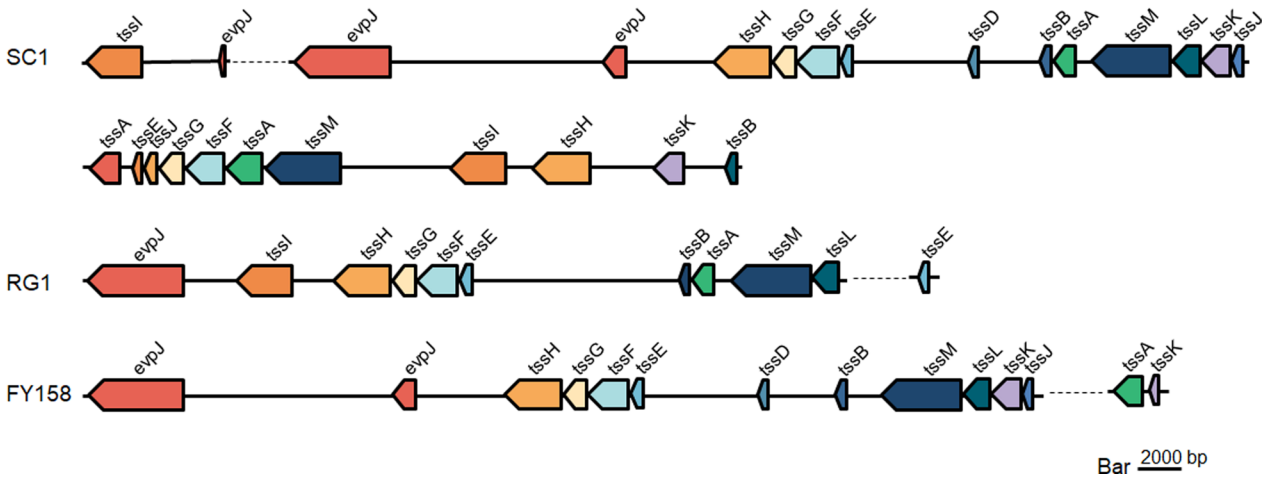

Fig. 4 Genetic organization of the T6SS clusters in strains SC1, RG1, and FY158. Genes are plotted as arrows in order according to their genomic positions in the T6SS gene cluster. The direction of each arrow indicates the gene coding strand, and the length of each arrow is in proportion to the size of the genes

Table 3 BGCs for the secondary metabolites identified in the genomes of SC1, RG1, and FY158

Metabolite	Similarity (%)	Gene loci		
		SC1	RG1	FY158
Microcin C7	71	–	–	900,947–922,005
Aerobactin	66	452,362–484,790	2,883,397–2,915,825	1,729,309–1,761,737
Deschlorosvetamycin A/svetamycin H/A	4	1,137,402–1,158,040	2,299,040–2,319,678	2,420,969–2,441,607
O-antigen	14	1,974,562–2,000,864	1,526,806–1,553,109	3,243,706–3,270,008
Enterobactin	100	2,304,051–2,357,719	1,164,731–1,218,406	3,562,637–3,616,314
Saquayamycin A	5	3,065,405–3,113,144	–	4,349,451–4,397,190
Aryl polyenes	100	3,849,334–3,892,927	4,251,366–4,294,959	–

"–" Denotes absent in the genome

(Fig. 5a), mutants *ΔiucC*, *ΔentF*, and *ΔentFΔiucC* exhibited impaired swimming motility, while the other three mutants showed no different swimming motility from wild-type SC1; all the mutants except *ΔentC* reduced biofilm formation (Fig. 5b). All the mutants significantly reduced antibacterial activity, with Δ*ape* and the *ΔentFΔiucC* double mutant displaying the most severe defects (Fig. 5c). Mutants Δ*ape*, *ΔentA*, *ΔentF*, and *ΔentFΔiucC* obviously attenuated virulence on rice leaves (Fig. 5d), with Δ*ape* and *ΔentFΔiucC* displaying the most severe defects. These findings highlight the pivotal roles of APEs, aerobactin, and enterobactin in the pathogenicity of *Enterobacter* in rice.

Discussion

During recent field surveys, we collected multiple samples of diseased rice leaves showing blight-like symptoms similar to those caused by *Xoo*. Despite repeated efforts,

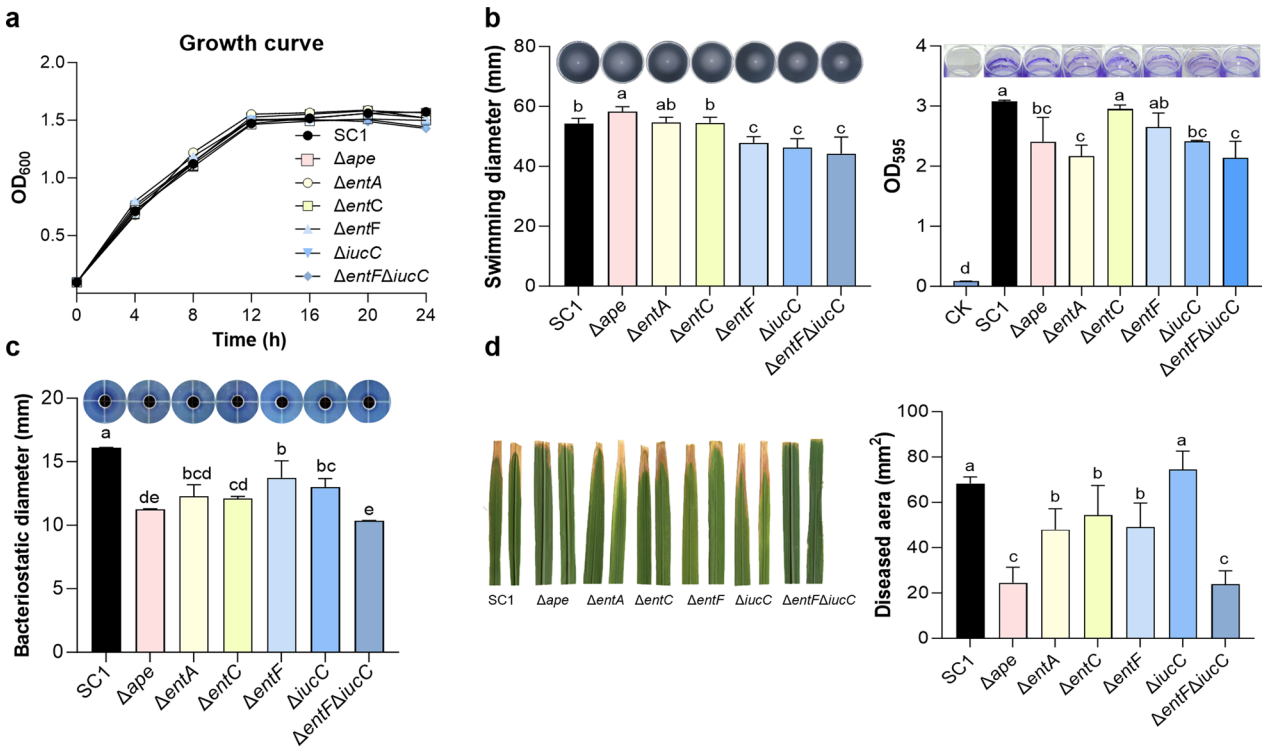

Fig. 5 Growth patterns, swimming motility, biofilm formation, antibacterial activity, and pathogenicity of SC1 and its mutants. **a** The growth curves of SC1 and its mutants in LB medium; **b** Swimming motility and biofilm formation of SC1 and its mutants; **c** Inhibitory effects of SC1 and its derivatives on *P. ananatis* SC7; **d** Pathogenicity of SC1 and its derivatives on rice leaves. Different lowercase letters indicate significant differences ($P < 0.05$)

we could not isolate *Xoo* from these samples. Instead, consistent isolation results identified bacterial colonies as members of *Enterobacter* (Xue et al. 2021; Yu et al. 2022). Therefore, *Enterobacter* is unlikely to be a secondary invader after *Xoo* infection. This conclusion is further supported by our inoculation results, which show that *Xoo* infection is not necessary for *Enterobacter* establishment. Notably, *Enterobacter* species are increasingly recognized as pathogens on various economically important plants, such as mulberry leaves wilt and peach fruit soft rot caused by *E. mori* (Zhu et al. 2011; Ahmad et al. 2021), onion bulb decay caused by *E. cloacae* (Zaid et al. 2011), rice bacterial palea browning, and sorghum bacterial leaf blight caused by *E. asburiae* (Cao et al. 2021; Chen et al. 2023). Despite these observations, the molecular mechanisms underlying the pathogenicity of *Enterobacter* to plants remain poorly understood due to limited research focus. To investigate their pathogenic mechanisms, we sequenced the complete genomes of three representative *Enterobacter* spp. strains, designated SC1, RG1, and FY158, isolated from Sichuan, Guangdong, and Zhejiang Provinces, respectively, and performed comparative genomic analyses. Phylogenetic classification revealed that SC1and FY158 belong to *E. pseudoroggenkampii*, while RG1 is an *E. asburiae* strain. In our previous study (Xue et al. 2021), strain SC1 was initially identified as *E. asburiae* based on multi-locus sequence analysis (MLSA) of housekeeping genes (e.g., *rpoB*, *gyrB*, etc.). In the present study, whole-genome sequencing and subsequent genomic analyses, including ANI, dDDH, and phylogenetic analysis, assigned SC1 to *E. pseudoroggenkampii*. This reclassification from *E. asburiae* to *E. pseudoroggenkampii* does not reflect an error in prior work but rather represents a taxonomic refinement enabled by more advanced genomic methods and alignment with current nomenclature standards. The updated classification ensures accuracy and consistency with contemporary understanding of *Enterobacter* phylogeny.

E. asburiae is typically recognized as an epiphytic bacterium, with some strains functioning as plant growth-promoting rhizobacteria (PGPR) (Liu et al. 2023; Ning et al. 2024; Tran et al. 2024), enhancing plant growth and stress resistance. However, recent studies have also identified *E. asburiae* as a pathogen responsible for rice bacterial palea browning (Cao et al. 2021), bacterial blight in rice (Yu et al. 2022) and sorghum (Chen et al. 2023), and radish tuber rot (Wang et al. 2023), underscoring its diverse pathogenic potential. To better understand the specific virulence genes unique to pathogenic *E. asburiae* isolates, a direct comparative genomic analysis between strain RG1 and PGPR isolates is essential. However, such analyses are currently constrained by the limited availability of genomic resources and published research on *E. asburiae*, particularly regarding well-characterized PGPR strains. Unlike *E. asburiae*, *E. pseudoroggenkampii* has, to our knowledge, only been reported in clinical samples (Wu et al. 2023). Our study represents the first isolation of *E. pseudoroggenkampii* from a plant host. Pathogenicity assays demonstrated that the traditional rice BB pathogen, *Xoo* PXO99^{A}, exhibited the highest virulence, followed by *E. asburiae* RG1, while *E. pseudoroggenkampii* SC1 and FY158 are the least pathogenic (Fig. 1). This variation may stem from differences in plant cell wall-degrading enzymatic activity between *Xoo* PXO99^{A} and the *Enterobacter* strains (Fig. 2a).

To better understand the pathogenic mechanisms of these bacterial strains, we conducted a comparative analysis of their virulence-associated secretion systems. The results revealed that strains FY158 and SC1 encode five distinct secretion systems (T1SS, T2SS, T4aP, T5SS, and T6SS), whereas RG1 carries only three (T2SS, T5SS, and T6SS) (Table 2). Notably, none of the strains possessed T3SS, a key virulence determinant in many plant pathogens (Deng et al. 2017). Intriguingly, all strains contained T6SS, with SC1 uniquely possessing two copies of this system. Given the well-established role of T6SS in bacterial competition and pathogenicity, and our observation that SC1 shows strong inhibitory activity against multiple pathogenic strains—particularly *Bacillus*, *P. ananatis*, and *Dickeya* (Fig. 2c)—we hypothesize that the dual sets of T6SS in SC1 may boost its competitive advantage against these microbes. This hypothesis will be a major focus of future research.

Our previous study demonstrated that strains SC1 and RG1 exhibit bacteriostatic activity against *Es. coli* DH5α (Xue et al. 2021). In the present study, these strains also inhibited the growth of pathogenic bacteria such as *P. ananatis*, *Dickeya*, and *Xanthomonas*, whereas the newly isolated strain FY158 showed only weak inhibition against two *Xanthomonas* strains (Fig. 2c). antiSMASH analysis suggested that the observed antibacterial activity may be linked to APEs, whose BGC is present in strains SC1 and RG1, but absent in strain FY158. APEs are commonly produced by host-associated bacteria, including commensals and pathogens of humans, animals, and plants, and are widespread among major bacterial genera within the *Proteobacteria* and *Bacteroidetes* (Cimermancic et al. 2014). Structurally, APEs resemble carotenoids, featuring an aryl group conjugated to a polyene carboxylic acid tail (Johnston et al. 2021). In Gram-negative bacteria, APEs are covalently anchored in the outer membrane, where they may modulate interactions with the surrounding environment. Functionally, APEs protect against photooxidative damage, akin to carotenoids (Schöner et al. 2014, 2016), and contribute to biofilm formation (Johnston et al. 2021). Given that biofilm

formation plays a crucial role in bacterial physiology, influencing pathogenicity and antibiotic resistance (Costerton et al. 1999), we sought to investigate the role of APEs in *Enterobacter* pathogenicity in rice. To this end, we generated an Δ*ape* mutant in strain SC1. Compared to the wild type, the Δ*ape* mutant exhibited significantly reduced antibacterial activity and pathogenicity (Fig. 5c, d), along with a slight increase in swimming motility (Fig. 5b). These findings identify APEs as important factors in the virulence of *Enterobacter* spp. during rice infection.

Aerobactin and enterobactin play pivotal roles in the virulence of *Enterobacter* on rice plants (Fig. 5d). Both siderophores are critical for iron acquisition, a function well-documented in various plant pathogens. For instance, siderophores have been implicated in fungal pathogens (Oide et al. 2006) as well as in bacterial species such as *Erwinia amylovora* (deferrioxamine) (Dellagi et al. 1998), *Pseudomonas syringae* (pyoverdine) (Taguchi et al. 2010), *Agrobacterium tumefaciens* (agrobactin) (Ong et al. 1979), and *D. dadantii* (achromobactin) (Münzinger et al. 2000).

Aerobactin, a citrate-hydroxamate siderophore, is produced by numerous pathogenic bacteria, including *Escherichia*, *Vibrio*, *Salmonella*, and *Shigella*, where it enhances virulence (Schçner et al. 2016). Beyond iron scavenging, aerobactin contributes to biofilm formation, oxidative stress resistance, and the detoxification of reactive oxygen species (ROS) (Li et al. 2022). Its biosynthesis is mediated by four genes (*iucABCD*), along with a transmembrane transporter gene (*iutA*). Enterobactin, another siderophore prevalent among *Enterobacterales*, functions as an antioxidant, aiding bacterial resistance to ROS and heavy metals (Holden et al. 2015). Notably, it is essential for *Pectobacterium atrosepticum* to establish plant infection (Gorshkov et al. 2021). In this study, deletion of the key biosynthetic genes of aerobactin (Δ*iucC*) and enterobactin (Δ*entF*) in SC1 significantly impaired bacterial motility, bacteriostatic activity, and pathogenicity (Fig. 5). These findings suggest that both siderophores contribute to virulence in *Enterobacter*-rice interactions, highlighting potential shared mechanisms among related pathogens. Further investigation is warranted to elucidate their precise roles in plant–pathogen dynamics.

Compared to each other, *Enterobacter* and *Xoo* use very different ways of causing disease. *Enterobacter* mainly depends on secondary metabolites, such as siderophores, which cause rice leaves to turn yellow and wither slowly, leading to a gradual progression of the disease. On the other hand, *Xoo* primarily utilizes the T3SS system to elicit a robust defense response from the host, accompanied by the intense degradation of rice leaf cell walls by enzymes such as Pel, Prt, and Cel, which enables disease lesions to expand rapidly.

It is indeed the core of the debate that *Enterobacter* strains contributing to leaf wilt are emerging pathogens or opportunistic colonizers. Unlike obligate pathogens, *Enterobacter* thrives in diverse environments (soil, water, decaying matter, insects), suggesting they are primarily opportunistic colonizers. However, changing conditions like extreme weather and intensive monoculture are now enabling some strains to emerge as significant pathogens, for example, the emergence of *E. asburiae* responsible for bacterial palea browning in rice, and bacterial leaf blight in rice and sorghum (Cao et al. 2021; Yu et al. 2022; Chen et al. 2023). Unlike dedicated pathogens such as *Pseudomonas syringae* or *Xoo*, *Enterobacter* lacks the full arsenal of specialized virulence (e.g., a T3SS), supporting its classification as an opportunistic pathogen. Another possibility is that *Enterobacter* acts not alone, but as a 'keystone pathogen' within a pathogenic consortium—a 'pathobiome'. It may modify the leaf environment (e.g., by breaking down plant defenses or altering the surface pH) to aid more virulent pathogens like *Xanthomonas* or *Pseudomonas*, leading to more severe disease. This idea warrants further validation.

Overall, the involvement of *Enterobacter* in leaf wilt indicates a significant change in plant disease dynamics. While not traditional primary pathogens, they represent a growing group of 'edge pathogens' that blur the line between opportunism and true pathogenicity. Their appearance signals ecosystem imbalance and highlights the adaptive potential of microbes. In summary, certain *Enterobacter* strains are opportunistic colonizers that are evolving into emerging pathogens.

Conclusions

In summary, our study is the first to identify *E. pseudoroggenkampii* as a causative agent of rice bacterial leaf wilt. We also provide the complete genome sequences of rice-derived *E. pseudoroggenkampii* and *E. asburiae*, and further demonstrate that aryl polyenes, and aerobactin and enterobactin phytotoxins serve as key virulence factors in rice-pathogenic *Enterobacter* strains. The high-quality genome assemblies presented here not only advance the understanding of *Enterobacter* pathogenesis but also offer a valuable genomic resource for future comparative studies.

Methods

Bacterial strains and growth conditions

The bacterial strains were isolated from rice plants infected with bacterial blight (BB)-like disease across different regions of China. Strain SC1 was obtained in June 2017 from Gaoshan Village, Chengdu City, Sichuan

Province; strain RG1 was collected in June 2020 from Daojiao Town, Dongguan City, Guangdong Province (Xue et al. 2021); and strain FY158 was isolated in May 2021 from Fuyang District, Hangzhou City, Zhejiang Province. All strains were maintained on LB medium (containing 10.0 g/L tryptone, 5.0 g/L yeast extract powder, 10.0 g/L NaCl, and 15 g/L agar for solid medium) at 37°C. For comparison, the reference strain *Xoo* PXO99^{A} was cultured at 30°C on NA medium (3 g/L beef extract, 5 g/L peptone, 10 g/L dextrose, and 15 g/L agar for solid medium).

Pathogenicity tests of the tested strains

In this study, we employed the clipping method (Yang and Bogdanove 2013) to assess the pathogenic potential of different bacterial strains on rice seedlings. The experiments were conducted using the rice cultivar 'Yuexiangzhan'. Before inoculation, seedling leaves were surface-sterilized with 70% ethanol and air-dried. Bacterial inoculum was prepared from overnight LB agar cultures grown at 37°C. Cells from individual cultures were scraped and resuspended in 15 mL of phosphate-buffered saline (PBS). The resulting suspensions were then adjusted to an optical density at 600 nm (OD_{600}) of 0.5 using a UV spectrophotometer. For inoculation, leaf tips (~ 1–2 cm in length) were clipped with scissors that had been dipped in bacterial suspension. After inoculation, the seedlings were transferred to an outdoor greenhouse maintained at an average temperature of 32°C. As a negative control, three sets of surface-sterilized rice seedlings were inoculated with PBS alone, while strain PXO99^{A} served as the positive control. Disease progression was evaluated 15 days post-inoculation (dpi), and the infected leaf area was quantified using ImageJ 1.52a (Schneider et al. 2012).

Growth curve measurement of the strains

A single colony of each bacterial strain grown on LB or NA plates was inoculated into 10 mL of LB or NB (NA without agar) broth and cultured overnight at 37°C with shaking at 200 rpm. Subsequently, the overnight culture was subcultured into fresh medium at a 1% inoculum ratio, and the OD_{600} was adjusted to approximately 0.01. The bacteria were incubated at 37°C with shaking at 200 rpm, and growth was monitored by sampling to measure the OD_{600} every 4 h.

Biochemical characteristic analysis of the strains

The biochemical properties of strains FY158, RG1, and SC1 were analyzed using Biolog GEN III microplates (bioMérieux) following the manufacturer's instructions. For chemotaxonomic analysis, exponentially growing cells of the three strains were cultivated in MB medium (TOPBIO, Shandong Tuopu Bioi-engineering Co., Ltd., Zhaoyuan, China) at 37°C for 3 days, harvested, and lyophilized. Cellular fatty acids were saponified, methylated, and extracted according to the Sherlock Microbial Identification System (MIDI) protocol. Fatty acid profiles were determined using an Agilent 7890B gas chromatography (Hewlett Packard, Santa Clara, USA) equipped with the Sherlock Microbial Identification software (version RTSBA6 6.21) and the Aerobic Bacterial Database.

Cell wall–degrading enzyme activity assay of the strains

The enzymatic activities of Cel, Pel, Peh, and Prt were determined using previously described methods (Lv et al. 2019; Xue et al. 2021) with minor modifications. The compositions of the assay media were as follows: Cel medium—1.0 g/L carboxymethyl cellulose, 3.8 g/L Na_3PO_4, and 8.0 g/L agarose (pH 7.0); Pel medium—10 g/L polygalacturonic acid, 10 g/L yeast extract, 0.1125 g/L $CaCl_2$, 100 mM Tris–HCl, and 8 g/L agarose (pH 8.5); Peh medium—5 g/L polygalacturonic acid, 2 g/L sucrose, 2.0 g/L $(NH_4)_2SO_4$, and 15 g/L agarose (pH 5.5); and Prt medium—LB medium supplemented with an equal volume of 1% (w/v) skimmed milk. For semi-quantitative assays, 5-mm diameter wells were punched into the agar plates, and 20 µL of bacterial culture (OD_{600} = 1.0) was added to each well. The plates were incubated at 37°C for the enzymatic reaction. After 12 h, the Pel and Peh assay plates were treated with 1 M HCl, while the Cel assay plate was stained with 0.1% Congo red followed by 1 M NaCl. The Prt assay plates were evaluated after 24 h without additional treatment, as proteolytic halos were directly visible. LB and PXO99^{A} were included as controls. All experiments were performed in triplicate.

Bacterial motility assay of the strains

The bacterial motility assay was performed as follows: fresh cultures (1 µL) of the target strains were individually spotted onto the center of a 90 mm semisolid plate containing 15 mL of swimming medium (5 g/L Bacto-Peptone, 5 g/L NaCl, and 3 g/L agar). The plates were then incubated at 37°C, and the diameters of the swimming motility zones were measured after 12 h of inoculation. Swarming assay was conducted using our previous studies (Lv et al. 2019; Xue et al. 2021). All experiments were conducted in triplicate with three independent replicates.

Biofilm formation assay

The bacteria were cultured in LB medium at 37°C with shaking at 200 rpm until OD_{600} = 1.0. Subsequently, 10 µL of each culture was transferred into 990 µL of SOBG

medium in individual wells of a 24-well polystyrene tissue culture plate. The plate was incubated at 37°C with shaking at 150 rpm for 48 h. After incubation, the medium was carefully aspirated, and the wells were stained with 1.5 mL of 0.1% (w/v) crystal violet solution. Unbound dye was removed by gently washing the wells three times with distilled water, followed by air-drying. To solubilize the biofilm-bound crystal violet, 2 mL of 95% ethanol was added to each well. Biofilm formation was quantified by measuring the absorbance at 595 nm using a multifunctional microplate reader (BioTek, USA). Each experiment was performed in quadruplicate.

Antibacterial assay of the strains

For the bacterial inhibition assay, 10 mL of molten LB agar was poured into a 9 cm square semisolid plate. After solidification, an overlay of 10 mL of 1% agarose (cooled to 50°C) supplemented with 100 µL of the selected bacterial culture ($OD_{600}=1.0$) was applied. The tested strains included *Bacillus velezensis* 3–10, *B. subtilis* H8, *Pantoea ananatis* SC7, *Dickeya zeae* MS2, *D. fangzhongdai* RY1, *Xoo* PXO99^{A}, and *X. axonopodis* Xac. Once the agarose layer had solidified, wells (5 mm in diameter) were punched, and 20 µL of FY158, RG1, or SC1 cultures ($OD_{600}=1.0$) were added to separate wells. The plates were incubated overnight at 30°C, and the diameter of inhibition zones was measured. All experiments were performed in triplicate.

Genome sequencing, assembly, and annotation of the strains

Genomic DNA was extracted from the SC1, RG1, and FY158 strains using the EasyPure Bacteria Genomic DNA Kit (TransGen Biotech, Beijing, China) according to the manufacturer's protocol. DNA quality was assessed by agarose gel electrophoresis, and quantified using a Qubit 2.0 Fluorometer (Thermo Scientific, Waltham, MA, USA). Whole genome sequencing was carried out on the Nanopore PromethION platform and Illumina MGISEQ T7 platforms by Grandomics Biosciences (Beijing, China).

For genome assembly, long-read data were processed using Flye v2.7, followed by polishing with both long- and short-read data using medaka v1.2.5 and pilon v1.2.3 (Wick et al. 2017), respectively. Genome annotation was performed using the NCBI PGAP pipeline (https://www.ncbi.nlm.nih.gov/genome/annotation_prok/) and eggNOG (http://eggnog-mapper.embl.de/). Additionally, BLAST comparisons were conducted against KEGG, GO, and SwissProt databases.

The complete genome sequences of SC1, FY158, and RG1 have been deposited in GenBank under accession numbers CP129025.1, CP129026.1, and CP129027.1, respectively.

Phylogenetic analysis and genomic comparison

Pairwise ANI values among strains SC1, RG1, and FY158, along with all 23 *Enterobacter* genomes available in the NCBI RefSeq database, were calculated using fastANI v1.3. Subsequently, dDDH values were determined using the Genome-to-Genome Distance Calculator (GGDC) 2.1 Web server (http://ggdc.dsmz.de/distcalc2.php) by uploading the genomic sequences (Meier-Kolthoff et al. 2013). For orthologous gene analysis, we employed OrthoFinder v2.5.4 with default parameters to cluster annotated proteins into orthogroups.

The BGCs potentially involved in the production of secondary metabolites, including phytotoxins, antibiotics, and antimicrobial compounds, were predicted using antiSMASH 7.0 (Blin et al. 2023).

Generation of in-frame deletion mutants

In-frame deletion mutants were generated via homologous recombination following the method described previously (Zhou et al. 2011). All primers used in this study are listed in Additional file 2: Table S6. First, the upstream and downstream fragments of the target genes were amplified using primer pairs gene-1/-2 and gene-3/-4, respectively, with SC1 genomic DNA as the template. These fragments were then fused by overlap PCR using primer pairs gene-1/-4. The resulting amplicons were purified and cloned into the *Bam*HI/*Spe*I-digested suicide plasmid pKNG101. The ligation products were transformed into *Es. coli* DH5α λpir competent cells, and recombinant constructs were verified by PCR amplification using pKNG101-F/-R primers. Subsequently, the verified plasmids were introduced into SC1 cells by triparental mating (Cheng et al. 2013) to generate in-frame mutants. Finally, the mutants were confirmed by DNA sequencing.

Statistical analysis

All values were presented as mean ± SD (n = 3 at least). Statistical comparisons between treatment groups were performed using two-way analysis of variance (ANOVA) in software R. A P-value ≤ 0.05 (95% confidence interval) was considered statistically significant for all analyses.

Abbreviations

ANI	Average nucleotide identity
ANOVA	Analysis of variance
APE	Aryl polyene
BB	Bacterial blight
BGC	Biosynthetic gene cluster
Cel	Cellulase
dDDH	Digital DNA-DNA hybridization
dpi	Days post-inoculation
ESKAPE	*Enterococcus faecium*, *Staphylococcus aureus*, *Klebsiella pneumoniae*,

	Acinetobacter baumannii, *Pseudomonas aeruginosa*, and *Enterobacter* spp.
GGDC	Genome-to-genome distance calculator
HTH	Helix-turn-helix
MFP	Membrane fusion protein
OD_{600}	Optical density at 600 nm
OMF	Outer-membrane pore protein
PBS	Phosphate-buffered saline
Peh	Polygalacturonase
Pel	Pectin lyase
PGPR	Plant growth-promoting rhizobacteria
Prt	Protease
ROS	Reactive oxygen species
T1SS	Type I secretion system
T2SS	Type II secretion system
T3SS	Type III secretion system
T4aP	Type IVa pilus
T5SS	Type V secretion system
T6SS	Type VI secretion system
VFDB	Virulence Factor Database
w/v	Weight/volume
Xoo	*Xanthomonas oryzae* pv. *oryzae*

Supplementary Information

The online version contains supplementary material available at https://doi.org/10.1186/s42483-025-00389-3.

Additional file 1: Figure S1. The growth curves of the three *Enterobacter* strains cultured in different media. **Figure S2.** Circular genome maps of SC1, RG1, and FY158. **Figure S3.** The biosynthesis gene clusters of secondary metabolites predicted in the genomes of SC1, RG1, and FY158.

Additional file 2: Table S1. Characteristics of strains FY158, RG1, and SC1. **Table S2.** The ANI values between SC1, RG1, FY158 genomes and the *Enterobacter* spp. genomes in the NCBI database. **Table S3.** Generalized database annotation statistics. **Table S5.** List of CDs unique to each strain. **Table S6.** Primers used in this study.

Additional file 3: Table S4. Putative virulence factors in strains SC1, FY158, and RG1 predicted against the Virulence Factor Database (VFDB).

Acknowledgements
We are very grateful to Dr. Yuxuan Hou in the China National Rice Research Institute, Hangzhou, China, for providing us with the FY158 strain.

Author contributions
JZ designed the experiments. FF, XY, XL, and MH performed the experiments. XZ, FF, and HC performed software-related work. FF and XY carried out validation and formal analysis. YX, XL, and JL conducted the investigation. YX, GS, and XQ provided resources. FF and XY were responsible for data curation. FF and XL wrote the original draft. JZ reviewed and edited the manuscript. FF prepared visualizations. JZ supervised the project. YD, TZ, and JZ acquired funding. All authors reviewed the results and approved the final version of the manuscript.

Funding
This work was supported by the grant from the National Key Research and Development Program of China (2022YFA1304400).

Availability of data and materials
The data presented in this study are openly available in NCBI database at https://www.ncbi.nlm.nih.gov/nuccore/NZ_CP129026.1, https://www.ncbi.nlm.nih.gov/nuccore/NZ_CP129027.1, and https://www.ncbi.nlm.nih.gov/nuccore/NZ_CP129025.1.

Declarations

Ethics approval and consent to participate
Not applicable.

Consent for publication
Not applicable.

Competing interests
The authors declare no competing interests.

Received: 29 May 2025 Accepted: 22 September 2025
Published online: 08 January 2026

References

Ahmad T, Ullah S, Moosa A, Liu Y, Nie C, Huang S. First report of preharvest soft rot of peach fruit (*Prunus persica*) caused by *Enterobacter mori* in China. Plant Dis. 2021;105(1):209.

Asolkar T, Ramesh R. The involvement of the type six secretion system (T6SS) in the virulence of *Ralstonia solanacearum* on brinjal. 3 Biotech. 2020;10(7):324. https://doi.org/10.1007/s13205-020-02311-4.

Baker JT, Allen LH, Boote KJ. Response of rice to carbon dioxide and temperature. Agric Forest Meteorol. 1992;60(3–4):153–66. https://doi.org/10.1016/0168-1923(92)90035-3.

Blin K, Shaw S, Augustijn HE, Reitz ZL, Biermann F, Alanjary M, et al. AntiSMASH 7.0: new and improved predictions for detection, regulation, chemical structures and visualisation. Nucleic Acids Res. 2023;51(W1):W46–50. https://doi.org/10.1093/nar/gkad344.

Cao P, Li C, Tan K, Zhao J, Wang X, Xiang W. Complete genomic data of *Enterobacter asburiae* strain SD4L associated with bacterial palea browning of rice in China. Plant Dis. 2021;105(12):4138–40. https://doi.org/10.1094/PDIS-03-21-0642-A.

Chen X, Laborda P, Li C, Zhao Y, Liu F. First report of bacterial leaf blight caused by *Enterobacter asburiae* on sorghum in Jiangsu province, China. Plant Dis. 2023;107(12):4017. https://doi.org/10.1094/PDIS-07-23-1325-PDN.

Cheng Y, Liu X, An S, Chang C, Zou Y, Huang L, et al. A nonribosomal peptide synthase containing a stand-alone condensation domain is essential for phytotoxin zeamine biosynthesis. Mol Plant Microbe Interact. 2013;26(11):1294–301. https://doi.org/10.1094/MPMI-04-13-0098-R.

Cimermancic P, Medema MH, Claesen J, Kurita K, Brown LCW, Mavrommatis K, et al. Insights into secondary metabolism from a global analysis of prokaryotic biosynthetic gene clusters. Cell. 2014;158(2):412–21. https://doi.org/10.1016/j.cell.2014.06.034.

Cosmas LL, Atong M, Poili E. Preliminary studies towards identification of ginger wilt disease in Sabah, Malaysia. Pertanika J Trop Agric Sci. 2016;39(3):373–80.

Costerton JW, Stewart PS, Greenberg EP. Bacterial biofilms: a common cause of persistent infections. Science. 1999;284(5418):1318–22. https://doi.org/10.1126/science.284.5418.1318.

Davin-Regli A, Lavigne JP, Pagès JM. *Enterobacter* spp.: Update on taxonomy, clinical aspects, and emerging antimicrobial resistance. Clin Microbiol Rev. 2019;32(4):e00002–19. https://doi.org/10.1128/CMR.00002-19.

Dellagi A, Brisset MN, Paulin JP, Expert D. Dual role of desferrioxamine in *Erwinia amylovora* pathogenicity. Mol Plant Microbe Interact. 1998;11(8):734–42. https://doi.org/10.1094/MPMI.1998.11.8.734.

Deng W, Marshall NC, Rowland JL, McCoy JM, Worrall LJ, Santos AS, et al. Assembly, structure, function and regulation of type III secretion systems. Nat Rev Microbiol. 2017;15(6):323–37. https://doi.org/10.1038/nrmicro.2017.20.

Gallegos-Monterrosa R, Coulthurst SJ. The ecological impact of a bacterial weapon: microbial interactions and the type VI secretion system. FEMS Microbiol Rev. 2021;45(6):fuab033. https://doi.org/10.1093/femsre/fuab033.

Gorshkov V, Parfirova O, Petrova O, Gogoleva N, Kovtunov E, Vorob'ev V, et al. The knockout of enterobactin-related gene in *Pectobacterium atrosepticum* results in reduced stress resistance and virulence towards the primed plants. Int J Mol Sci. 2021;22(17):9594. https://doi.org/10.3390/ijms22179594.

Hoffmann H, Stindl S, Stumpf A, Mehlen A, Monget D, Heesemann J, et al. Description of *Enterobacter ludwigii* sp. nov., a novel *Enterobacter* species of clinical relevance. Syst Appl Microbiol. 2005;28(3):206–12. https://doi.org/10.1016/j.syapm.2004.12.009.

Holden VI, Bachman MA. Diverging roles of bacterial siderophores during infection. Metallomics. 2015;7(6):986–95. https://doi.org/10.1039/c4mt00333k.
Huang X, Kurata N, Wei X, Wang ZX, Wang A, Zhao Q, et al. A map of rice genome variation reveals the origin of cultivated rice. Nature. 2012;490(7421):497–501. https://doi.org/10.1038/nature11532.
Johnston I, Osborn LJ, Markley RL, McManus EA, Kadam A, Schultz KB, et al. Identification of essential genes for *Escherichia coli* aryl polyene biosynthesis and function in biofilm formation. Npj Biofilms Microbi. 2021;7(1):56. https://doi.org/10.1038/s41522-021-00226-3.
Lau YY, Yin WF, Chan KG. *Enterobacter asburiae* strain L1: complete genome and whole genome optical mapping analysis of a quorum sensing bacterium. Sensors (Basel). 2014;14(8):13913–24. https://doi.org/10.3390/s140813913.
Lee SW, Han M, Park CJ, Seo YS, Bartley LE, Jeon JS. The molecular mechanisms of rice resistance to the bacterial blight pathogen, *Xanthomonas oryzae* pathovar *oryzae*. In Advances in botanical research. Academic Press. 2011;60: 51–87. https://doi.org/10.1016/B978-0-12-385851-1.00002-0.
Li EF, Tian XL, Zhao RB, Wang YH, Wang G. First report of *Enterobacter cloacae* causing bulb decay on garlic in China. Plant Dis. 2022;106(1):310. https://doi.org/10.1094/PDIS-05-21-0972-PDN.
Liu F, Hu M, Tan X, Xue Y, Li C, Wang S, et al. *Pseudomonas chlororaphis* L5 and *Enterobacter asburiae* L95 biocontrol dickeya soft rot diseases by quenching virulence factor modulating quorum sensing signal. Microb Biotechnol. 2023;16(11):2145–60. https://doi.org/10.1111/1751-7915.14351.
Liu F, Yang J, Xiao Y, Li L, Yang F, Jin Q. Complete genome sequence of a clinical isolate of *Enterobacter asburiae*. Genome Announc. 2016;4(3):e00523-e616. https://doi.org/10.1128/genomeA.00523-16.
Liu W, Liu J, Triplett L, Leach JE, Wang GL. Novel insights into rice innate immunity against bacterial and fungal pathogens. Annu Rev Phytopathol. 2014;52:213–41. https://doi.org/10.1146/annurev-phyto-102313-045926.
Lv M, Hu M, Li P, Jiang Z, Zhang LH, Zhou J. A two-component regulatory system VfmlH modulates multiple virulence traits in *Dickeya zeae*. Mol Microbiol. 2019;111(6):1493–509. https://doi.org/10.1111/mmi.14233.
Meier-Kolthoff JP, Auch AF, Klenk HP, Göker M. Genome sequence-based species delimitation with confidence intervals and improved distance functions. BMC Bioinform. 2013;14:60. https://doi.org/10.1186/1471-2105-14-60.
Mew TW, Alvarez AM, Leach JE, Swings J. Focus on bacterial blight of rice. Plant Dis. 1993;77:5–12. https://doi.org/10.1094/PD-77-0005.
Mizukami T, Wakimoto S. Epidemiology and control of bacterial leaf blight of rice. Annu Rev Phytopathol. 1969;7(1):51–72. https://doi.org/10.1146/annurev.py.07.090169.000411.
Münzinger M, Budzikiewicz H, Expert D, Enard C, Meyer JM. Achromobactin, a new citrate siderophore of *Erwinia chrysanthemi*. Z Naturforsch C. 2000. https://doi.org/10.1515/znc-2000-5-605.
Z Naturforsch C J Biosci. 2000;55(5–6): 328–32. https://doi.org/10.1515/znc-2000-5-605.
Naqvi SAH. Bacterial leaf blight of rice: An overview of epidemiology and management with special reference to-Indian-sub-continent. PJAR. 2019;32(2):359. https://doi.org/10.1758/journal.pjar/2019/32.1.59.72.
Ning Z, Lin K, Gao M, Han X, Guan Q, Ji X, et al. Mitigation of salt stress in rice by the halotolerant plant growth-promoting bacterium *Enterobacter asburiae* D2. J Xenobiot. 2024;14(1):333–49. https://doi.org/10.3390/jox14010021.
Oide S, Moeder W, Krasnoff S, Gibson D, Haas H, Yoshioka K, et al. NPS6, encoding a nonribosomal peptide synthetase involved in siderophore-mediated iron metabolism, is a conserved virulence determinant of plant pathogenic ascomycetes. Plant Cell. 2006;18(10):2836–53. https://doi.org/10.1105/tpc.106.045633.
Ong SA, Peterson T, Neilands JB. Agrobactin, a siderophore from *Agrobacterium tumefaciens*. J Biol Chem. 1979;254(6):1860–5. https://doi.org/10.1016/S0021-9258(17)37736-0.
Schçner TA, Gassel S, Osawa A, Tobias NJ, Okuno Y, Sakakibara Y, et al. Aryl polyenes, a highly abundant class of bacterial natural products, are functionally related to antioxidative carotenoids. ChemBioChem. 2016;17(3):247–53. https://doi.org/10.1002/cbic.201500474.
Schneider CA, Rasband WS, Eliceiri KW. NIH image to ImageJ: 25 years of image analysis. Nat Methods. 2012;9(7):671–5. https://doi.org/10.1038/nmeth.2089.
Schroeder BK, Waters TD, Du Toit LJ. Evaluation of onion cultivars for resistance to *Enterobacter cloacae* in storage. Plant Dis. 2010;94(2):236–43. https://doi.org/10.1094/PDIS-94-2-0236.
Schöner TA, Fuchs SW, Schönau C, Bode HB. Initiation of the flexirubin biosynthesis in *Chitinophaga pinensis*. Microb Biotechnol. 2014;7(3):232–41. https://doi.org/10.1111/1751-7915.12110.
Schöner TA, Gassel S, Osawa A, Tobias NJ, Okuno Y, Sakakibara Y, et al. Aryl polyenes, a highly abundant class of bacterial natural products, are functionally related to antioxidative carotenoids. ChemBioChem. 2016;17(3):247–53. https://doi.org/10.1111/1751-7915.12110.
Taguchi F, Suzuki T, Inagaki Y, Toyoda K, Shiraishi T, Ichinose Y. The siderophore pyoverdine of *Pseudomonas syringae* pv. *tabaci* 6605 is an intrinsic virulence factor in host tobacco infection. J Bacteriol. 2010;192(1):117–26. https://doi.org/10.1128/JB.00689-09.
Tran TD, Lee SI, Hnasko R, McGarvey JA. Biocontrol of *Escherichia coli* O157:H7 by *Enterobacter asburiae* AEB30 on intact cantaloupe melons. Microb Biotechnol. 2024;17(3):e14437. https://doi.org/10.1111/1751-7915.14437.
Wang R, Wang X, Liu Y, Chen P, Wang Y, Wang W, et al. First report of radish tubers rot caused by *Enterobacter asburiae* in China. Plant Dis. 2023;107(9):2839. https://doi.org/10.1094/PDIS-11-22-2650-PDN.
Wick RR, Judd LM, Gorrie CL, Unicycler KH. Resolving bacterial genome assemblies from short and long sequencing reads. PLoS Comput Biol. 2017;13(6):e1005595. https://doi.org/10.1371/journal.pcbi.1005595.
Wu S, He Y, Feng Y, Zong Z. *Enterobacter pseudoroggenkampii* sp. nov. carrying quinolone-resistant gene qnrE recovered from clinical samples in China. Antonie Van Leeuwenhoek. 2023;116(7):643–51. https://doi.org/10.1007/s10482-023-01833-0.
Xue Y, Hu M, Chen S, Hu A, Li S, Han H, et al. *Enterobacter asburiae* and *Pantoea ananatis* causing rice bacterial blight in China. Plant Dis. 2021;105(8):2078–88. https://doi.org/10.1094/PDIS-10-20-2292-RE.
Yang B, Bogdanove A. Inoculation and virulence assay for bacterial blight and bacterial leaf streak of rice. Methods Mol Biol. 2013;956:249–55. https://doi.org/10.1007/978-1-62703-194-3_18.
Yang D, Zhao L, Li Q, Huang L, Qin Y, Wang P, et al. The involvement of the T6SS *vgrG* gene in the pathogenicity of *Pseudomonas plecoglossicida*. J Fish Dis. 2023;46(10):1097–108. https://doi.org/10.1111/jfd.13829.
Yu L, Yang C, Ji Z, Zeng Y, Liang Y, Hou Y. First report of new bacterial leaf blight of rice caused by *Pantoea ananatis* in southeast China. Plant Dis. 2022;106(1):310. https://doi.org/10.1094/PDIS-05-21-0988-PDN.
Zaid AM, Bonasera JM, Beer SV. First report of *Enterobacter* bulb decay of onions caused by *Enterobacter cloacae* in New York. Plant Dis. 2011;95(12):1581. https://doi.org/10.1094/PDIS-05-11-0375.
Zhang M, Zhang Y, Han X, Wang J, Yang Y, Ren B, et al. Whole genome sequencing of *Enterobacter mori*, an emerging pathogen of kiwifruit and the potential genetic adaptation to pathogenic lifestyle. AMB Express. 2021;11(1):129. https://doi.org/10.1186/s13568-021-01290-w.
Zhou J, Zhang H, Wu J, Liu Q, Xi P, Lee J, et al. A novel multidomain polyketide synthase is essential for zeamine production and the virulence of *Dickeya zeae*. Mol Plant Microbe Interact. 2011;24(10):1156–64. https://doi.org/10.1094/MPMI-04-11-0087.
Zhu B, Lou MM, Xie GL, Wang GF, Zhou Q, Wang F, et al. Enterobacter mori sp. Nov., associated with bacterial wilt on Morus alba L. Int J Syst Evol Micr. 2011;61(11):2769–827. https://doi.org/10.1099/ijs.0.028613-0.